Preliminary Geologic Map of the Canjilon SE Quadrangle, Rio Arriba County, New Mexico.

By

Kirt Kempter, Kate Zeigler, Dan Koning, and Spencer Lucas

May 2007

New Mexico Bureau of Geology and Mineral Resources
Open-file Digital Geologic Map OF-GM 150

Scale 1:24,000

This work was supported by the U.S. Geological Survey, National Cooperative Geologic Mapping Program (STATEMAP) under USGS Cooperative Agreement 06HQPA0003 and the New Mexico Bureau of Geology and Mineral Resources.

New Mexico Bureau of Geology and Mineral Resources
801 Leroy Place, Socorro, New Mexico, 87801-4796

Geology of the 7.5-Minute Canjilon SE Quadrangle, Abiquiu Region, Northcentral New Mexico

by:

Kirt Kempter, Kate Zeigler, Dan Koning and Spencer Lucas

Southwestern Flank of Sierra Negra
Black Mesa and the Sangre de Cristo Mountains in the background

Geologic mapping of the Canjilon SE 7.5-Minute Quadrangle was funded by the New Mexico Bureau of Geology and Mineral Resources STATEMAP Program and the USGS National Cooperative Geologic Mapping Program.

Geologic Overview

Geologic mapping of the Canjilon SE 7.5-minute quadrangle was conducted in the second half of 2006 and early 2007. The quadrangle is located north of the Chama River along the boundary of the Abiquiu embayment (western Rio Grande Rift) and the Colorado Plateau. Cañon de Cobre, a wide north-south trending canyon floored by late Paleozoic Cutler Group sediments and rimmed by early Mesozoic Chinle Group sediments, occupies much of the southwestern portion of the quadrangle. The northern quarter of Cañon de Cobre makes a dogleg bend to the northeast, following a northeast trend in structural grain. The axis of a faulted, southwest-plunging anticline trends through Cañon de Cobre, with Colorado Plateau sediments dipping gently to the southwest on the west side of the axis and to the southeast on the east side of the axis (Figure 23). East of Cañon de Cobre, Tertiary El Rito, Ritito, and Abiquiu Formations cap the older sequence, dipping southeasterly into the rift and offset by numerous north- and northeast-trending faults.

In the northwest corner of the quadrangle, a thick sequence of Mesozoic sediments is preserved, including several Triassic and Jurassic formations. These rocks are part of a prominent northeast-trending escarpment that originates near Ghost Ranch. The Upper Triassic Poleo Sandstone forms a resistant bench across much of the eastern margin of the Colorado Plateau as backwasting of the Mesozoic sediments occurred in the Tertiary. In the Canjilon SE quadrangle, this topographic escarpment also existed during deposition of the Ritito Conglomerate, which filled low topography south and adjacent to the escarpment on the Poleo sandstone bench. As Ritito Conglomerate sediments accumulated along the paleoescarpment, colluvial debris from Mesozoic sediments (in particular Jurassic Entrada sandstone) was incorporated into Ritito Conglomerate sediments as the paleovalley filled.

Several mafic igneous rocks are exposed in the quadrangle, yielding clues to the timing of volcano-tectonic episodes in the rift. Three samples were collected for geochronologic analyses, including a mafic dike on the western escarpment of Cañon de Cobre, the Cerrito de la Ventana dike north of Plaza Blanca, and a mafic lava flow capping Sierra Negra. The mafic dike in Cañon de Cobre yielded an age of 18.1±1.2 Ma,

while the Cerrito de la Ventana dike gave an age of 18.9±0.41 (see Appendix II). Both of these age determinations were derived from groundmass concentrates and yielded somewhat disturbed results. Still, they are in close agreement with ages determined for these units from a geologic study of the Abiquiu 7-5-minute quadrangle by Maldonado (2008).

The mafic lava sample collected from lava-capped Sierra Negra yielded an age of 5.00±0.15, a result with high precision (see Appendix II). This lava preserves a thick sequence of Abiquiu Formation sediments overlain by Chama-El Rito Formation. The sample was collected from the basal flow of 3 flows, each exhibiting a brecciated top and bottom (Figure 8). Phreatomagmatic deposits, including a well-exposed vent on the northwest flank of Sierra Negra, occur within the Chama-El Rito Formation and may be related to 15-16 Ma vents to the east (El Rito quadrangle) adjacent to Hwy 554 (Maldonado, 2008).

Broad Quaternary terraces define the northeastern and eastern margins of the quadrangle. These terraces suggest a complex history of erosion and deposition in the Quaternary, including multiple shifts in outflow directions for Madera Creek.

Key Observations and Results

The list below emphasizes the key observations and interpretations made during the course of this mapping project.

1. Mapping of the Ritito Conglomerate provides a much better understanding of its distribution and the paleotopographic setting of the area during its deposition. Distinctive metarhyolite boulders (often granitic in appearance) with blue-gray, rounded quartz crystals are prevalent in deposits in the northern half of the quadrangle but are rare in deposits to the south. They possibly originated from Proterozoic highs near Ojo Caliente, including Cerro Colorado, where similar metarhyolites occur in situ today. In general, clast size in the Ritito Conglomerate decreases to the south, but also becomes more angular and

diverse in Proterozoic igneous and metamorphic compositions. Possibly, these clasts originated from a (now buried) range of Proterozoic rocks that extended southward from Cerro Colorado, Ojo Caliente. A third Proterozoic source for Ritito Conglomerate deposits is from the Sierra Nacimiento Mountains to the southwest (Timmer et al., 2006). These sediments, which include Paleozoic limestone clasts, do not appear to have reached the Canjilon SE area. In the northwest corner of the quadrangle, a paleotopographic escarpment is being exhumed by erosion. Presumably, early rift tectonism precipitated Ritito Conglomerate sedimentation and began to fill a large paleovalley adjacent to a northeast-trending escarpment of Mesozoic sediments. Quaternary erosion has exhumed this escarpment, with remnants of the paleovalley fill (Ritito Conglomerate) extending to the southwest onto the Colorado Plateau.

2. Exposures along the eastern wall of upper Arroyo Hondo suggest that most Mesozoic rocks were stripped by erosion from the eastern portion of the quadrangle prior to the deposition of the El Rito Formation. An irregular topography existed in the western portion of the quadrangle at this time, with El Rito Formation deposits resting in angular unconformity on a variety of tilted Mesozoic units, including Upper Triassic Chinle Group and Middle Jurassic Entrada Formation. Cobbles, boulders and other clasts in the El Rito Formation are significantly more rounded and mature than in the Ritito Conglomerate, implying a higher energy fluvial system.
3. Exposures of Triassic Poleo Formation in the western rim of Cañon de Cobre show syndepositional deformation of sandstone beds (Figure 18). Deformation likely occurred along thin Salitral shale beds above undeformed Shinarump Formation sandstones and conglomerates. Such deformation may explain tilted, unusual Poleo Formation structures in the Youngsville quadrangle (Kelley et al., 2005).
4. Sierra Negra is capped by at least 3 mafic lava flows but there is no vent at the peak. Lavas in the peak area cap middle Miocene Chama-El Rito sandstone and phreatomagmatic deposits. The peak of Sierra Negra (just off the quadrangle) is flanked by eastern and southwestern basalt-capped mesas. The

peak basalt flow dips moderately to the west, making this flow contiguous with the capping basalt of the west mesa. A major basaltic dike just north of Sierra Negra (UTM 0387500, 4015500) may be a source of these flows. A thick pile of basalt on the northeastern flank of Sierra Negra (El Rito quadrangle) may also represent a plug or source vent. Major landslide detachments characterize much of the western flank of Sierra Negra.

5. Mapping of the quadrangle identified numerous rift-related faults. The Cañones fault, which enters the quadrangle in the southwestern corner, veers northeast, then more easterly, crossing the eastern rim of Cañon de Cobre. Other northeast-trending faults continue to the north along the eastern rim of Cañon de Cobre, representing a broken anticlinal axis - that also marks the boundary of the Colorado Plateau and the Rio Grande Rift. East of this axis the entire sequence dips to the southeast, with numerous down-to-the-northwest minor faults.
6. Madera Creek, the main drainage from highlands to the north, has had a complex Quaternary history. The highest Quaternary terrace in the northeast portion of the quadrangle (traversed by FR-137), likely formed as the Madera Creek drainage curved eastwards toward Pine Canyon Tank. A slightly younger and lower terrace formed as Madera Creek changed course to flow more southerly, forming a broad terrace named Llano Blanco. During the Holocene, Madera Creek incised its modern drainage along the east and northeast margin of Llano Blanco.
7. Although the modern creekbed of Madera Creek is well established, headward erosion of Cañon de Cobre (to the northeast) appears destined to pirate Madera Creek in the near geologic future. Just 1 km northeast of the head of Cañon de Cobre, Madera Creek skirts the canyon, flowing at an elevation of ~7,900 feet. The floor of Cañon de Cobre in the vicinity, however, is already less than 7,400', approximately 500 feet lower than the unsuspecting Madera Creek.
8. A catastrophic Quaternary (?) flooding event in an unnamed tributary canyon to Cañon de Cobre (east and northeast of Las Minas de Jimmie) is believed to have emplaced giant Proterozoic quartzite boulders measuring 2-5 meters in diameter,

scattered across the valley floor and hill slopes of this canyon. Any accompanying sedimentary deposits related to these boulders were not observed, presumably removed by erosion, leaving the giant boulders as lag (see photos in unit descriptions below).

Unit Descriptions for the Canjilon SE 7.5-minute Quadrangle

The oldest rocks in the Canjilon SE quadrangle belong to the El Cobre Canyon Formation of the Cutler Group and are Late Pennsylvanian to Early Permian in age. Mesozoic rocks include a variety of Late Triassic to Middle Jurassic strata, while Cenozoic rocks include the Tertiary El Rito Formation, Ritito Conglomerate, and Abiquiu Formation. Early to Late Miocene mafic volcanism is also preserved in the quadrangle, either as mesa-capping lava flows on Sierra Negra, or as dikes related to Rio Grande rift tectonics. This section provides a description of each of the major rock groups in the quadrangle, with a schematic stratigraphic chart shown below (Figure 1).

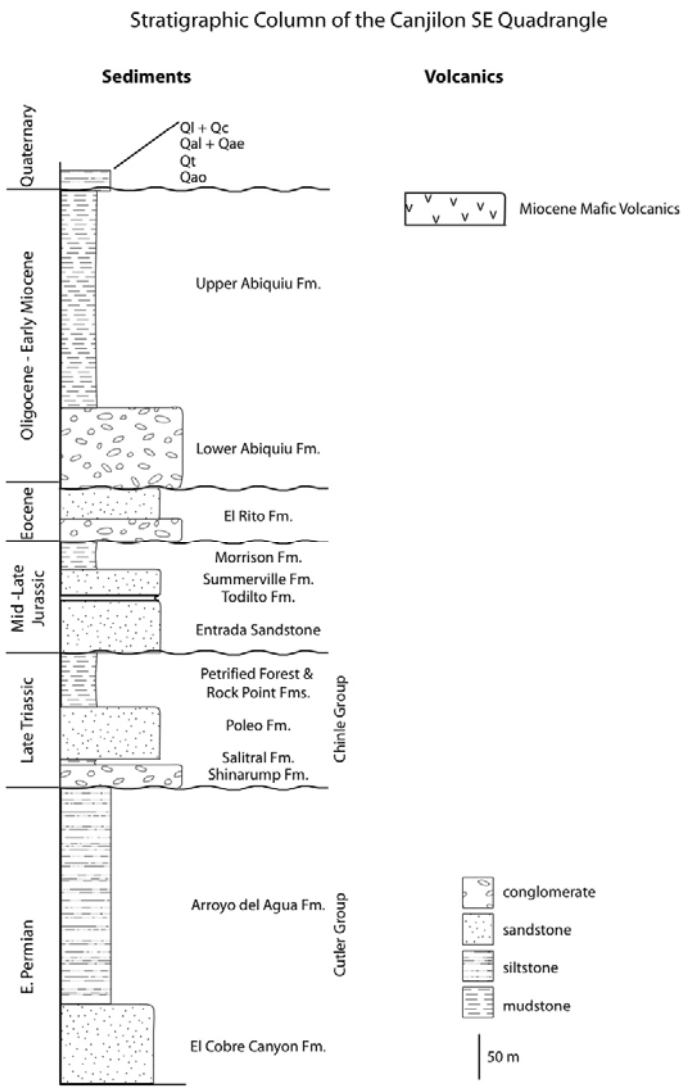

Figure 1. Stratigraphic column for the Canjilon SW quadrangle.

Quaternary Units

Qa – Alluvium. Late Pleistocene to Holocene. Alluvial deposits in modern drainage bottoms and elevated basins. Deposits include conglomerates, sands, and silts. Holocene terrace deposits less than 2 meters above drainage bottoms are also included. Maximum thickness is estimated to be less than 5 meters.

Qae – Alluvium. Late Pleistocene to Holocene. Same as Qa but with a significant eolian sand component. Fine- to medium-grained sand. Thickness less than 2 meters.

Qc – Colluvium. Late Pleistocene to Holocene. Poorly sorted talus, debris, and other rock fragments derived from local volcanic and sedimentary rocks. Often occurs as wedge-shaped hillslope deposits (Figure 2). The poorly consolidated Ritito Conglomerate is typically expressed at the surface as colluvial clasts and often obscures the contact with the El Rito Formation below. Also, cobble and boulder alluvial facies of the El Rito Formation produce significant colluvium. Clasts from both the Ritito Conglomerate and the El Rito Formation form extensive colluvial lag on hillslopes throughout the central and eastern areas of the quadrangle. Although pervasive throughout the quadrangle, colluvium was seldom mapped. Maximum thickness is approximately 8 meters.

Figure 2. Quaternary colluvium and landslide debris on Permian Arroyo del Agua Formation in the north rim of Cañon de Cobre.

Qac – Alluvium and Colluvium. Late Pleistocene to Holocene. Mix of alluvial and colluvial deposits, mostly on low angle slopes. Maximum thickness is estimated to be less than 2 meters.

Ql (Qly, Qlm, Qlo, Qlb) – Landslides. Pleistocene to Holocene. Unsorted, chaotic debris emplaced during a single detachment event from a steep slope or cliff, generally containing a sediment matrix. Also, slump or block slides, especially along the flanks of steep hillslopes such as the slopes of Cañon de Cobre and Sierra Negra. Qlb represents landslide material composed dominantly of blocks of basalt. Fan-shaped deposits occur where debris spread out on valley floor. On the western flank of Sierra Negra, the relative ages of major landslide events are indicated by Qly (youngest), Qlm (intermediate), and Qlo (oldest). Thickness can exceed 20 meters.

Qlc – Landslides plus Colluvium. Pleistocene to Holocene. Mix of colluvium and landslide material, mostly on the flanks of Sierra Negra. Maximum thickness is approximately 5 meters.

Qt (Qt1, Qt2, Qt3, Qt4) – Terrace deposits. Pleistocene to Holocene. Alluvial deposits near the margins of modern streams or older perched floodplain deposits. Holocene, low terraces (< 10 meters above modern drainages) are typically fill deposits of sand, silt and gravel, and are mapped as Qt. Ancestral versions of Madera Creek and its tributaries are believed to have created several strath terraces as Quaternary erosion in the Rio Chama valley progressed. The highest and oldest terrace is labeled Qt1. Accordingly, the youngest and lowest terrace is labeled Qt4. These terraces typically are characterized by 1 to 3 meters of alluvial sand to conglomerate, capping tilted and beveled Tertiary strata. Maximum thickness is <5 meters.

Qao – Alluvium. Late Pleistocene to Holocene. Mapped in the Cañon de Cobre area where it is older than Qa in the canyon and in the NW portion of the quadrangle. Sandy alluvial beds with minor gravel and muddy beds preserved as terrace-like features on top

sandstone benches and capping Tertiary units. Thicknesses range from 0.5 m to almost 2 m. Usually more heavily vegetated than Qa units.

Qg – Alluvium. Middle to Late Pleistocene. Alluvial gravels that cap hills along the western and southern rims of Cañon de Cobre. Deposits include reworked and remobilized Tr deposits. Sandy pebble and conglomerate lenses with lesser amounts of silt and mud. Maximum thickness is approximately 2 m.

Giant quartzite boulders – Though not a map unit, in a major (but unnamed) tributary to Cañon de Cobre east and northeast of Las Minas Jimmie, occur numerous Proterozoic quartzite boulders that exceed 2 meters across and rest upon the canyon floor and slopes. The boulders are subrounded to angular, are uniformly quartzite in composition, and range between 2-5 meters in diameter (Figures 3-5). Were there any other evidence of glaciation in the area they might be interpreted as glacial erratics. They are particularly prevalent on Chinle Poleo Formation dip slopes approximately 1 km northeast of Las Minas Jimme. Like glacial erratics, they typically occur in clusters or as isolated boulders with no other associated gravels or sedimentary deposits. They are unrelated to the Tertiary El Rito Formation, Ritito Conglomerate, or Abiquiu Formation, which do not include quartzite boulders of this size in the Canjilon SE quadrangle.

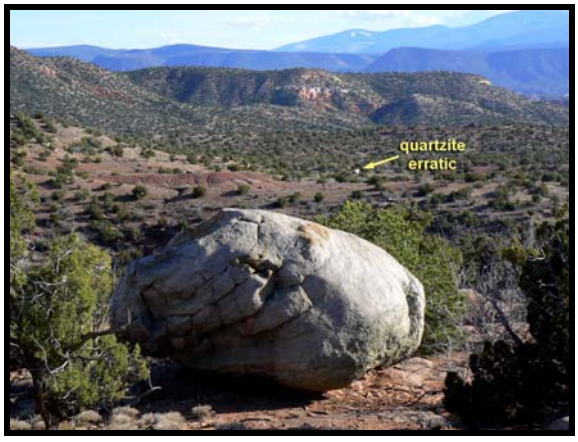

Quartzite boulders (foreground and distance)

Cluster of quartzite boulders with backpack for scale.

Figure 3. Giant quartzite bouders found scattered along the eastern margin of Cañon de Cobre.

Figure 4. Quartzite boulder at least 5 meters across.

Figure 5. Cluster of quartzite boulders, each more than 3 meters in diameter.

The origin of these quartzite boulders is unclear, but most likely were transported during a catastrophic Quaternary flood, with the boulders traveling a significant distance from a source north of the quadrangle, near primary Proterozoic quartzite outcrops of the Tusas Mountains. Water was their likely transport method, as no known glacial deposits occur in the Abiquiu area or the Tusas Mountains. The fact that Cañon de Cobre is such a large canyon today with no perennial stream hints that such a flood may have been an important factor in the early formation of the canyon. The boulders likely remain as lag material, with the smaller alluvial fractions removed by erosion over time. Timing of this flooding event is also unclear, since the boulders occur on hillslopes and on the valley floor, but probably occurred during the Quaternary. Their isolated nature and random distribution preclude them as a mappable unit, but several UTM locations for individual bouldera are provided below:

UTM 0381041, 4014202 • UTM 0380865, 4016070 • UTM 0380389, 4016280
UTM 0381289, 4016451 • UTM 0381839, 4016451

Tb, Tbi – Mafic volcanic rocks. Late Oligocene to Early Miocene. Dark gray to black mafic lavas or dikes. Lavas are generally crystal-poor, with phenocrysts of olivine and plagioclase (less than 5%). Dikes are similarly crystal-poor, although a mafic dike that traverses the western rim of Cañon de Cobre (Figure 6) contains abundant olivine phenocrysts. Cerritos de la Ventana is a major dike that intruded a northeast-trending fault plane. In places the dike splits, forming two parallel strands. Along the north and northwestern flanks of Sierra Negra, mafic dikes intrude the Abiquiu Formation (Figure 7) while mafic lavas cap a western mesa (on the quadrangle) and eastern mesa (off the quadrangle). A major basaltic dike just north of Sierra Negra (UTM 0387500, 4015500) may be a source of these flows. The eastern mesa includes at least 3 successive flows occur with brecciated basal horizons. An $^{40}Ar/^{39}Ar$ sample from the lowest flow yielded an age of 5.0±0.15 Ma (Appendix II). To the

west there is only one flow. Maximum thickness of flow on the western mesa of Sierra Negra is approximately 15 meters.

Figure 6. Basaltic dike in the western wall of Cañon de Cobre. Kate Ziegler for scale.

Figure 7. Dike cutting Abiquiu Formation on northwest side of Sierra Negra.

Figure 8. Three lava flows separated by breccia horizons on east mesa of Sierra Negra (off quadrangle. Note pink exposure of paleosol on Chama-El Rito Formation at the base of lowermost lava (lower right of photo).

Ttc (Ttcp) – Chama-El Rito Member, Tesuque Formation, Santa Fe Group. Miocene. Light pink to reddish brown floodplain deposits of siltstone, mudstone, fine-grained sandstone and thin channels of low-angle crossbedded channel gravels. Fluvial channels contain rounded volcanic pebbles of intermediate and felsic composition, poorly to moderately sorted. These channels are typically cemented by calcium carbonate. Exposures occur only on the flanks of Sierra Negra. Brownish phreatomagmatic deposits are intercalated with the regular sediments, containing bombs and other altered tephra of mafic composition (Figure 9). A large phreatomagmatic crater is well preserved on the north flank of Sierra Negra (Figure 10). Maximum thickness is approximately 185 meters.

Figure 9. Volcanic bomb and phreatomagmatic deposits in the Chama-El Rito member.

Figure 10. Phreatomagmatic crater deposits (Ttcp) on north flank of Sierra Negra. Geologist Dan Koning for scale.

Ta – Abiquiu Formation. Late Oligocene to Early Miocene. White to beige fine-grained tuffaceous sandstones with interbedded shales and fluvial conglomerates that contain pebbles or cobbles of volcanic rocks and Proterozoic quartzites (Figure 11). The distinctive bedding and presence of 25.1 Ma Amalia Tuff clasts and other Ar^{40}/Ar^{39} age data indicate that the bulk of Abiquiu sedimentation occurred as pumiceous debris flow deposits coincident with the eruption of the Questa caldera along with pre- and post-caldera volcanism in the Latir volcanic field. (Smith et al., 2002). Porphyritic dacites, including phenocrysts of plagioclase and hornblende are the most common clast, although a variety of silica-rich lavas and tuffs occur as clasts. To the north this unit correlates with the Cordito Member of the Los Pinos Formation. In the study area the unit fines upwards with increasing volcaniclastic material. Maximum thickness is approximately 350 meters.

Figure 11. Abiquiu Formation on the southwestern flank of Sierra Negra, dipping to the southeast.

Tr – Ritito Conglomerate. Late Oligocene. Alluvial conglomerate and sandstone. Gray to pink fluvial deposits, commonly conglomeratic and arkosic, due to pink metavolcanic and granitic clasts. Typically poorly consolidated with a calcified base up to 1 meter thick (Figure 12). Clasts include subequal amounts of quartzite and metarhyolite, with lesser amounts of schist, gneiss, vein quartz, and granite. The deposit is characteristic of a widespread piedmont alluvial fan derived from Proterozoic source regions. Previously, this unit was defined as the lower member of the Abiquiu Formation, however Maldonado and Kelley (2009) proposed to distinguish this unit based on its unique composition and age. The poorly bedded nature of the deposit is suggestive of a depositional environment of braided streams and debris flows. In the northern half of the quadrangle clasts in the conglomerate are typically subrounded to rounded (up to 0.7 meters across), consisting of Proterozoic metarhyolite and metasediments (in particular blue-gray quartzite). To the south the gravels and conglomerates become subangular to

angular and include a wider variety of Proterozoic clasts. The larger, subrounded granite and quartzite boulders diminish in abundance to the south. Maximum thickness is approximately 60 meters.

Figure 12. Calcified base of Ritito Conglomerate with a wide variety of granitic and metamorphic clasts. Lithified horizon typically less than 2 meters.

Te -- El Rito Formation. Eocene. Siltstones, sandstones and conglomerates. Alluvial deposits dominated by quartzite conglomerate and quartzose sandstone (Figure 13). Lesser amounts of siltstone and mudstone. Basal conglomerate is typically clast supported with subrounded to rounded bluish gray cobbles to boulders. This basal unit was deposited on an irregular erosional surface of older Late Paleozoic to Mesozoic strata (Figure 14). The sandstone units represent sheet-flow and channel-fill sediments in a braided stream environment. The age of these sediments is regarded to be Eocene (Logsdon, 1981; Smith et al., 1961) and the unit is thought to have been deposited in syn-orogenic basin between Laramide highlands in the Sierra Nacimiento to the west and the Tusas Mountains to the northeast. The sandstone units represent sheet-flow and channel-

fill sediments in a braided stream environment. Maximum thickness is approximately 50 meters.

Figure 13. Channel sandstone above conglomerate in the El Rito Formation.

Figure 14. Channel of El Rito Formation basal conglomerate carved into the Jurassic Entrada sandstone. Note the well rounded, mature quartzite cobbles and boulders. Silicified fault plane crossing the basal conglomerate of the El Rito Formation.

Jurassic stratigraphy on the Ghost Ranch quadrangle follows Lucas et al. (2005a), which is based on the regional stratigraphy of Anderson and Lucas (1992, 1994, 1995, 1996, 1997) and Lucas and Anderson (1997, 1998).

Jmb -- Brushy Basin Member of the Morrison Formation. Upper Jurassic. Variegated pale greenish gray, grayish yellow green, pale olive, yellowish brown, and pale reddish brown bentonitic mudstone with a few beds of trough-crossbedded pebbly sandstone. Locally, the base of the Morrison Formation is a thin (up to 8 m thick) interval of trough-crossbedded sandstone and interbedded mudstone. Above that interval, the formation is mostly mudstone. Greenish white, medium-bedded sandstones with cross-bedding and mud rip-up clasts and thin tabular sandstones are present in a few places near the top of the unit. The basal sandy interval is likely correlative to the Salt Wash Member of the Morrison Formation to the west and south. However, this interval is neither thick enough, persistent enough, nor lithologically distinctive enough to separate from the Brushy Basin Member. 41 m to 68 m thick.

Jt -- Todilto Formation. Middle Jurassic. Limestone and gypsum. The Todilto Formation consists of a lower, limestone-dominated interval (Luciano Mesa Member) overlain locally by a gypsum interval (Tonque Arroyo Member) (Lucas et al., 1985, 1995; Kirkland et al., 1995). The Luciano Mesa Member is 2 to 5 m thick and consists mostly of thinly laminated, dark gray or yellowish gray, kerogenic limestone. Beds near the base of the member are usually sandy, and microfolding of the thin limestone laminae is common. Thickness is less than 5 meters.

Je -- Entrada Sandstone. Middle Jurassic. Trough crossbedded and ripple laminated, cliff-forming sandstone. The Entrada Sandstone (only the Slick Rock Member is present in the Abiquiu region: Lucas et al., 2005a). The unit is very fine- to medium-grained, moderately well sorted sandstone that forms bold cliffs along escarpments and mesa tops. Trough crossbeds and ripple laminations are the dominant bedforms. Coloration is typically orangy-red base, beige middle, and yellow top. Up to 50 m thick.

Triassic Units

All Triassic strata in the quadrangle are assigned to the Upper Triassic Chinle Group (Lucas, 1993). The Chinle Formation was first named and described by Gregory for exposures in the Chinle Valley of northwestern Arizona. Triassic stratigraphy in the Jarosa quadrangle follows Lucas and Hunt (1992) and Lucas et al. (2003, 2005b). Three informal units are mapped at the 1:24,000 scale.

TRcu – Petrified Forest and Rock Point Formations. Poorly exposed, thinly bedded pink to white shales, siltstones, and sandstones. Much of the backwasting of younger Mesozoic strata and cliffs across the eastern Colorado Plateau margin is due to this unit. Sandstone and conglomerate lenses are discontinuous and are more prevalent near the top of the unit. The best exposures of this unit in the quadrangle are west of Rincón Amarillo along the northern boundary of the quadrangle (Figure 15). Maximum thickness ~30 meters.

Figure 15. Shales of the Petrified Forest Formation near Rincón Amarillo at the northern quadrangle boundary. Discontinuous sandstone and conglomerate lenses towards the top.

TRcp – Poleo Formation. Yellow-brown, medium to fine-grained, micaceous, cross-bedded, quartzose sandstone, conglomeratic sandstone and conglomerate (Figures 16-18). Planar and trough cross stratification common. Layers containing abundant petrified wood fragments are common (Figure 16). The conglomerate in the Poleo Formation is often dark brown and contains both intrabasinal siltstone and nodular calcrete clasts and extrabasinal siliceous (chert and quartzite) clasts. This unit forms prominent cliffs, in particular along the rim of Cañon de Cobre. The base of the unit is sharp (corresponds to the Tr-4 unconformity of Lucas (1993)) and the upper contact is gradational into the

overlying Painted Desert Member of the Petrified Forest Formation. Maximum thickness is approximately 65 meters.

Figure 16. Wood frament fossils in Poleo Formation sandstone.

Figure 17. Kate Zeigler resting on Poleo Formation sandstone along the northern rim of Cañon de Cobre. Sierra Negra is on the left side and the Jemez Mountains form the horizon.

Figure 18. Syndepositional deformation of Poleo sandstone beds in the western rim of Cañon de Cobre. Deformed beds are underlain by undeformed sandstones and conglomerates of the Shinarump Formation and are overlain by undeformed beds of upper Poleo Formation sandstone.

TRcl – Shinarump and Salitral Formations. The basal unit of the Chinle Group is called the Shinarump Formation (previously called the Agua Zarca Formation) and consists of white, coarse-grained to medium-grained pebbly sandstone with conglomeratic lenses (Figure 19). Low to medium scale channel crossbeds are common. Extrabasinal conglomerate includes clasts of quartz, chert, and quartzite. Where well exposed, the base of the unit disconformably overlies the Permian Arroyo del Agua Formation of the Cutler Group. Locally there is copper mineralization, consisting of copper sulfides that have replaced carbonaceous material and are surrounded by halos of copper carbonates (Figure 20). Some petrified wood and plant fragments. Maximum thickness is exposed in the northern wall of Cañon de Cobre, where a Shinarump channel is ~25 meters thick.

Locally, thin beds of the Salitral Formation overlie the Shinarump Formation along the western and northern rims of Cañon de Cobre. The Salitral Formation is a reddish-brown to mottled shale that is thin, discontinuous and poorly exposed. Due to its poor surface representation, this unit was only mapped in a few locations. Most likely, syndepositional deformation of overlying Poleo sandstone beds occurred along a detachment surface across Salitral shale beds (Figure 18). Maximum thickness is approximately 7 meters.

Figure 19. Shinarump Formation conglomerate lens with extrabasinal fluvial clasts.

Figure 20. Copper mine in Shinarump Formation sandstone. Notice azurite and malachite on boulder to the bottom left of the mine entrance.

Late Pennsylvanian to Early Permian Units

The oldest strata exposed on the Canjilon SE quadrangle are Late Pennsylvanian to Early Permian siliciclastic red beds of the Cutler Group (Cutler Formation of Smith et al., 1961). These strata are particularly well exposed in the Cañon del Cobre (Figure 21). Lucas and Krainer (2005) divided Cutler strata into two, mappable lithostratigraphic units, the El Cobre Canyon and Arroyo del Agua formations. A measured section through the Cutler Group is provided below (Figure 22), with field measurements detailed in Appendix I. Several lithologic criteria allow the two formations to be distinguished:

El Cobre Canyon Formation	**Arroyo del Agua Formation**
"brown" (pale reddish brown—10 R 5/4)	"orange" (moderate reddish brown—10 R 4/6)
extraformational conglomerates (quartzite, granite, gneiss clasts)	few conglomerates except uppermost beds; most other conglomerates are intraformational (calcrete clasts)
most beds calcareous to very calcareous	most beds not calcareous
multistoried sandstone beds	thin sandstone sheets
thin siltstone slopes	thick siltstone slopes
rhizoliths common	calcrete nodules very abundant

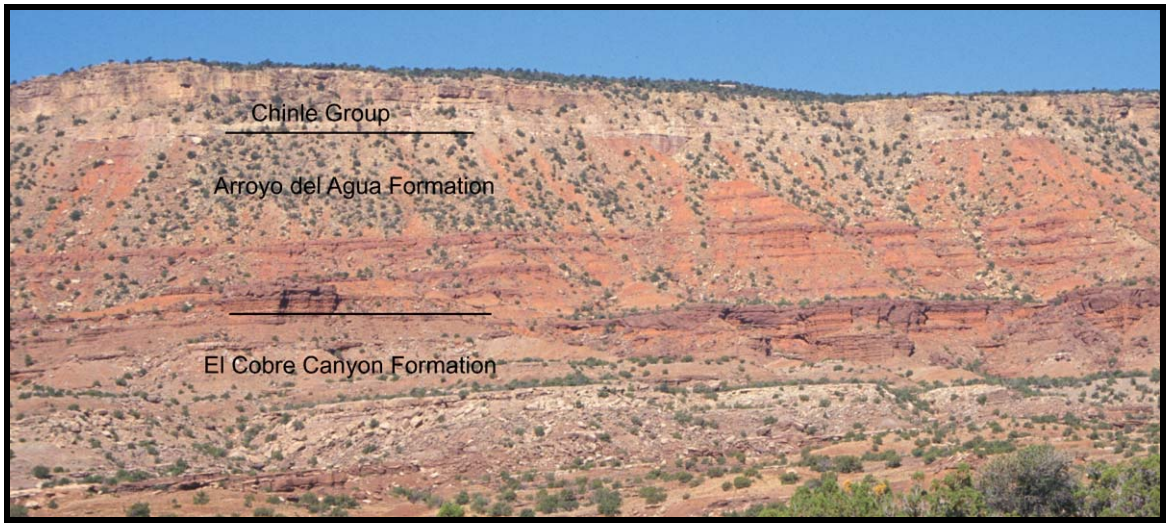

Figure 21. Western rim of Cañon de Cobre showing Cutler Group contacts.

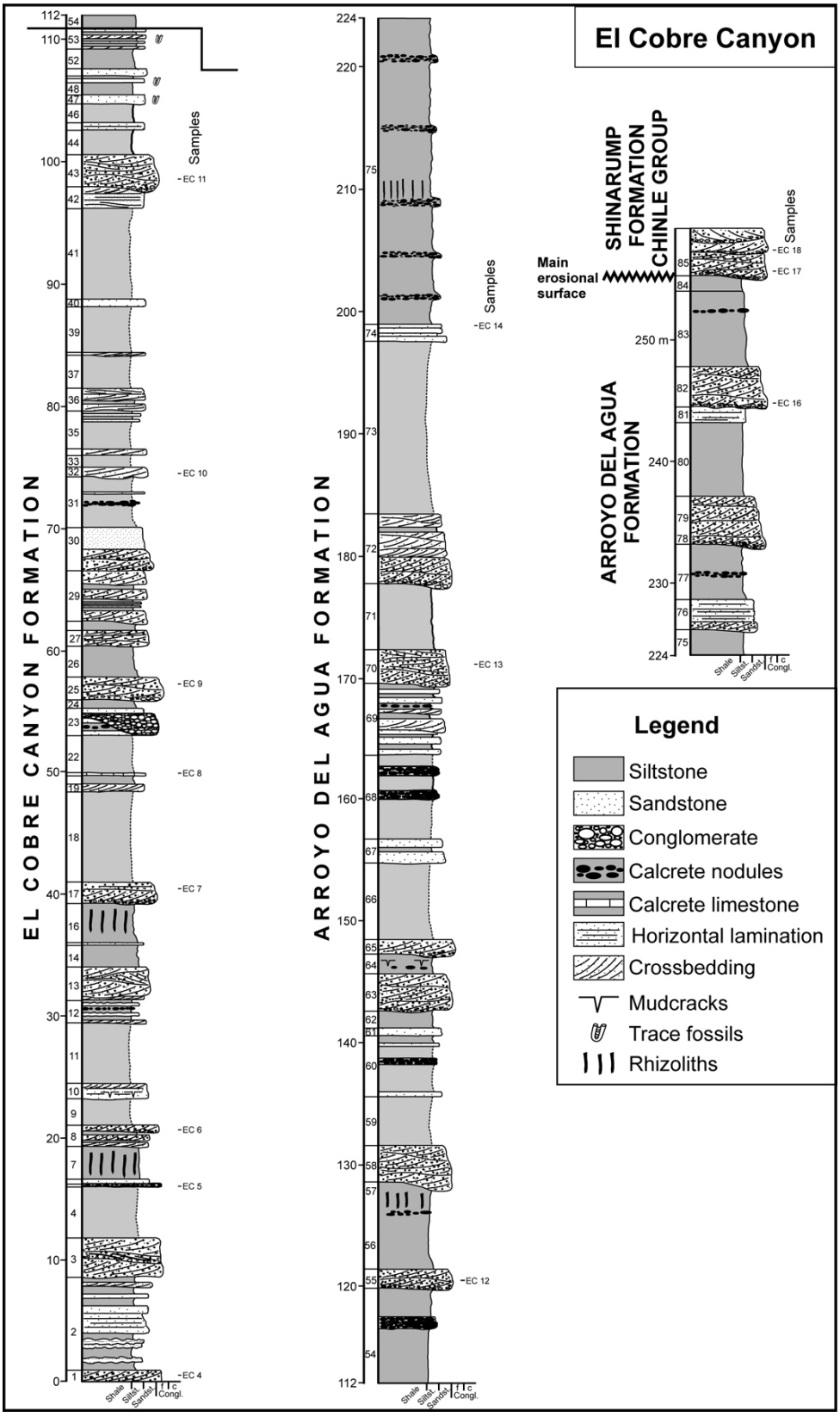

Figure 22. Cutler Group measured section

Pcu -- Arroyo del Agua Formation. Early Permian. Orange siltstone, sandstone and minor intraformational and extraformational conglomerate. The siltstones are thick, slope-forming units with abundant calcrete nodules between thin sandstone sheets that are arkosic and trough crossbedded. Up to 130 m thick.

Pcl -- El Cobre Canyon Formation. Late Pennsylvanian-Early Permian. Brown siltstone, sandstone and extraformational conglomerate that overlies Proterozoic basement in the subsurface and is conformably overlain by the Arroyo del Agua Formation. Siltstone beds of the El Cobre Canyon Formation contain numerous rhizoliths and comprise relatively thin, slope-forming units between multistoried sandstone beds that are arkosic, micaceous, coarse grained and trough crossbedded. On the Canjilon SE quadrangle, contains numerous vertebrate fossils, primarily of Late Pennsylvanian-Early Permian amphibians and reptiles (e.g., Langston, 1953; Berman, 1993; Lucas et al., 2005b). At least 111 m thick.

Structure

The structural boundary between the Colorado Plateau and the Rio Grande rift passes through the Canjilon SE quadrangle. The focus of detachment is represented by a SSE-plunging anticline whose axis is broken by northeasterly faults parallel to the eastern rim of Cañon de Cobre (Figure 23). From the west, Colorado Plateau sediments ramp up gently to the anticlinal axis, dipping to the southwest. East of the axis, these sediments dip to the southeast (into the rift) and are overlain by younger El Rito Formation, Ritito Conglomerate, and Abiquiu Formation.

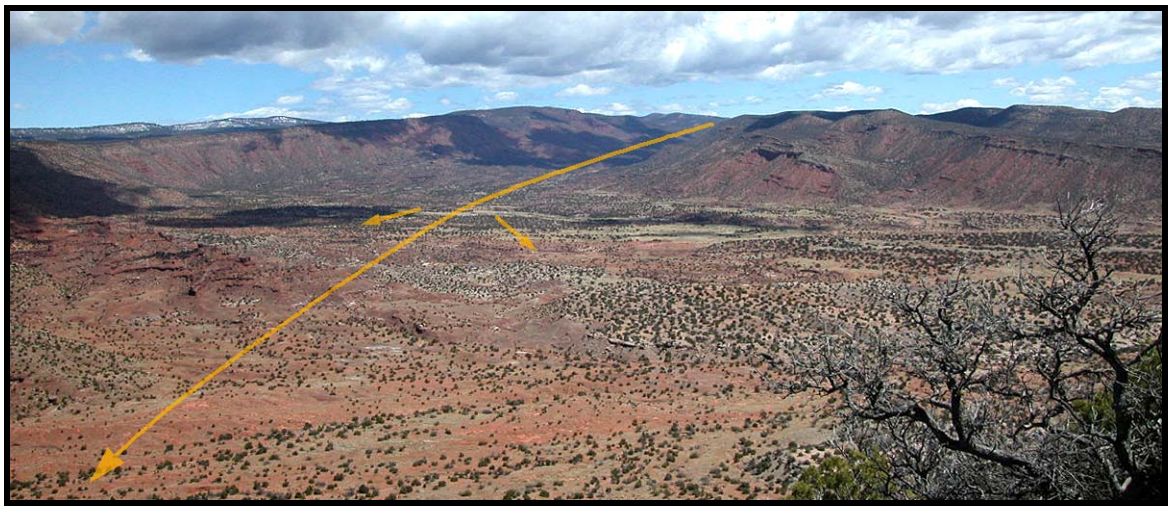

Figure 23. View looking north up Cañon de Cobre. Note westerly dip of strata on western canyon rim (left side of photo) and easterly dip of strata on the eastern rim. The axis of a faulted, southwesterly-plunging anticline trends parallel and adjacent to the eastern canyon rim.

The accompanying cross section to this report traverses the quadrangle from northwest to southeast, roughly perpendicular to the dominant northeast-trending structural grain. In the far northwest corner of the quadrangle Jurassic strata (Entrada, Todilto, Morrison) overlie the Late Triassic Chinle Group, with Cretaceous strata just off the quadrangle, capping the Mesozoic sequence. Severe erosion during the Laramide, however, removed most of the Jurassic and Cretaceous from the area prior to deposition of the Eocene El Rito Formation. Even the resistant Chinle Poleo Formation was removed in places (possibly the majority of the eastern half of the quadrangle). East of Madera Creek El Rito Formation rests upon Permian Arroyo del Agua Formation.

The majority of the faults in the eastern portion of the quadrangle are down-to-the-west, with typically less than 50 meters of offset. The persistant southeastern dip, however, preserves younger deposits, such as the Abiquiu Formation and Chama-El Rito Formation in the upper parts of Sierra Negra. The Cañones Fault enters the quadrangle in the southwestern corner, and gradually bends eastward as it crosses the Cañon de Cobre valley floor. Excellent exposures of the fault are preserved in Upper Red Wash Canyon and locally in the valley floor (Figures 24 and 25). Offset along the fault diminishes to the east. East of Cañon de Cobre the fault begins to curve northward again, changing offset direction.

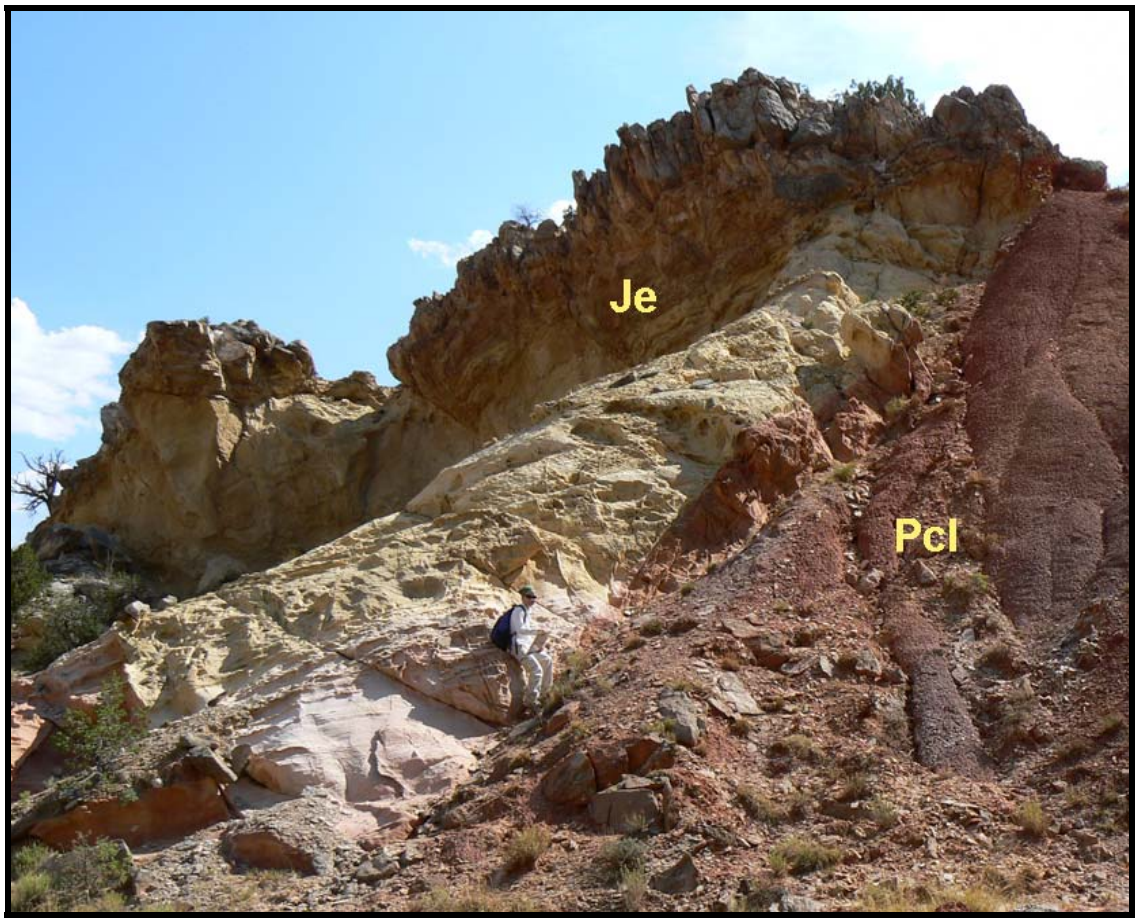

Figure 24. Cañones fault contact between Jurassic Entrada (Je) and Late Pennsylvanian to Early Permian El Cobre Canyon Formation (Pcl). Upper Red Wash Canyon.

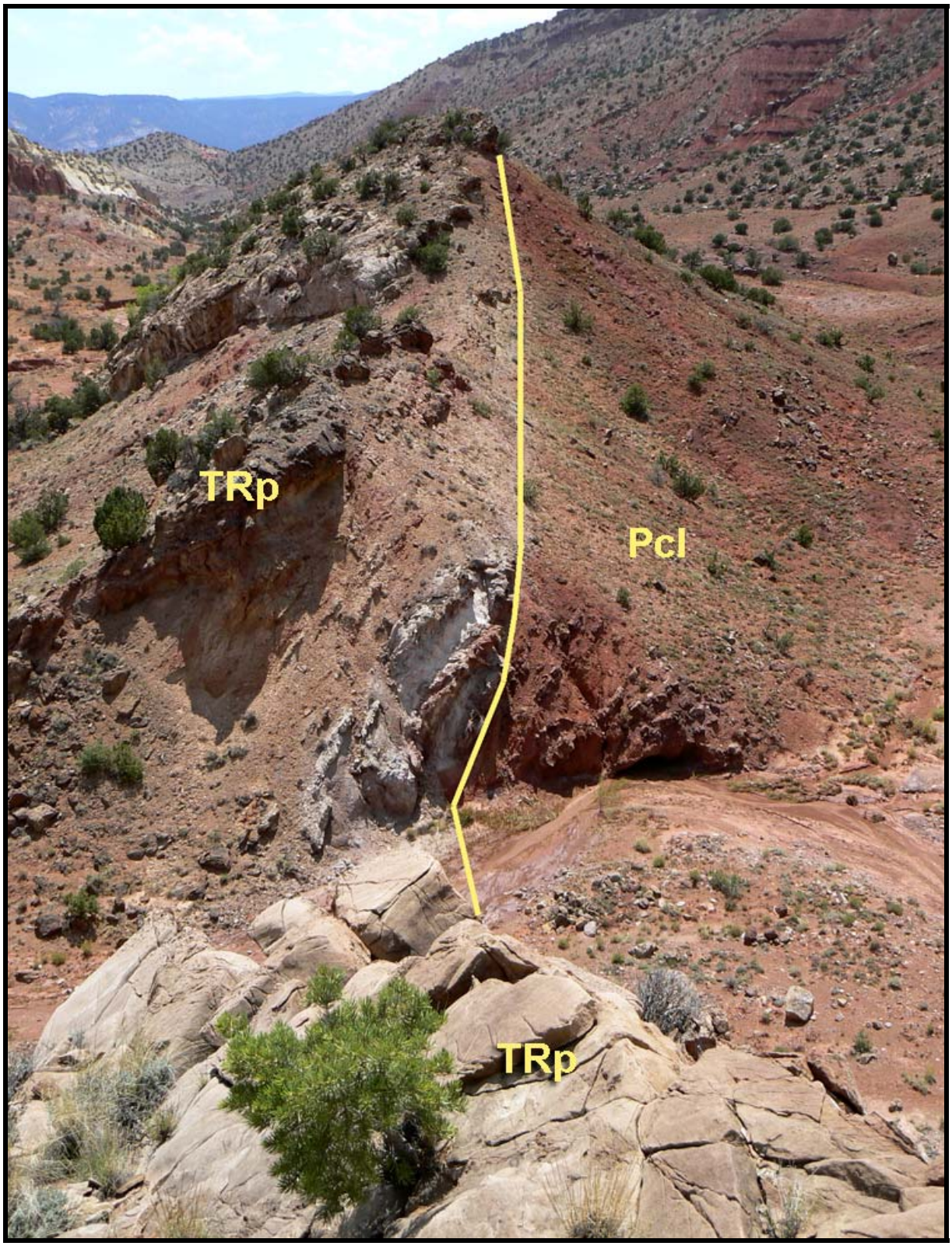

Figure 25. Cañones fault in the floor of Cañon de Cobre, juxtaposing Early Triassic Poleo Formation (TRp) with Late Pennsylvanian to Early Permian El Cobre Canyon Formation (Pcl).

REFERENCES

Anderson, O. J., and Lucas, S. G., 1992, The Middle Jurassic Summerville Formation, northern New Mexico: New Mexico Geology, v. 14, p. 79-92.

Anderson, O. J., and Lucas, S. G., 1994, Middle Jurassic stratigraphy, sedimentation and paleogeography in the southern Colorado Plateau and southern High Plains; *in* Caputo, M. V., Peterson, J. A., and Franczyk, K. J., eds., Mesozoic systems of the Rocky Mountain region: Denver, RMS-SEPM, p. 299-314.

Anderson, O. J., and Lucas, S. G., 1995, Base of the Morrison Formation, Jurassic, of northwestern New Mexico and adjacent areas: New Mexico Geology, v. 17, p. 44-53.

Anderson, O. J., and Lucas, S. G., 1996, Stratigraphy and depositional environments of Middle and Upper Jurassic rocks, southeastern San Juan Basin, New Mexico: New Mexico Geological Society, Guidebook 47, p. 205-210.

Anderson, O. J., and Lucas, S. G., 1997, The Upper Jurassic Morrison Formation in the Four Corners Region: New Mexico Geological Society, Guidebook 48, p. 139-155.

Berman, D. S., 1993, Lower Permian vertebrate localities of New Mexico and their assemblages: New Mexico Museum of Natural History and Science, Bulletin 2, p. 11-21.

Dubiel, R.F., 1989, Depositional environments of the Upper Triassic Chinle Formation in the eastern San Juan Basin and vicinity, New Mexico: U.S. Geological Survey, Bulletin 1808B, p. 1-22.

Kempter, K.A., Kelley, S.A., and Lawrence, J.R., (2007) The geology of the northern Jemez Mountains, North-central New Mexico. New Mexico Geological Society Guidebook, v. 58.

Kelley, S.A., Lawrence, J.R., and Osburn, G.R., 2005, Preliminary geologic map of the **Youngsville** 7.5-minute Quadrangle, Rio Arriba County, New Mexico, New Mexico Bureau of Geology and Mineral Resources, Open-file Geologic Map OF-GM 106, scale 1:24,000.

Kirkland, D.W., Denison, R.E., and Evans, R., 1995, Middle Jurassic Todilto Formation of northern New Mexico and southwestern Colorado: Marine or nonmarine?: New Mexico Bureau of Mines and Mineral Resources, Bulletin 147, 37 p.

Langston, W., Jr., 1953, Permian amphibians from New Mexico: University of California, Publications in Geological Sciences, v. 29, p. 349-416.

Logsdon, M.J., 1981, A preliminary basin analysis of the El Rito Formation (Eocene), north-central New Mexico: Geological Society of America Bulletin, v. 92

Lucas, S.G., 1993, The Chinle Group: Revised stratigraphy and biochronology of Upper Triassic strata in the western United States: Museum of Northern Arizona, Bulletin, v. 59, p. 27-50.

Lucas, S. G., and Anderson, O. J., 1997, The Jurassic San Rafael Group, Four Corners region: New Mexico Geological Society, Guidebook 48, p. 115-132.

Lucas, S.G. and Anderson, O.J., 1998, Jurassic stratigraphy and correlation in New Mexico: New Mexico Geology, v. 20, p. 97-104.

Lucas, S.G., and Hunt, A.P., 1992, Triassic stratigraphy and paleontology, Chama Basin and adjacent areas, north-central New Mexico: New Mexico Geological Society, Guidebook 43, p. 151-167.

Lucas, S. G. and Krainer, K., 2005, Stratigraphy and correlation of the Permo-Carboniferous Cutler Group, Chama Basin, New Mexico: New Mexico Geological Society, Guidebook 56, p. 145-159.

Lucas, S. G., Anderson, O. J., and Pigman, C., 1995, Jurassic stratigraphy in the Hagan basin, north-central New Mexico: New Mexico Geological Society, Guidebook 46, p. 247-255.

Lucas, S. G., Hunt, A. P. and Spielmann, J., 2005a, Jurassic stratigraphy in the Chama Basin, northern New Mexico: New Mexico Geological Society, Guidebook 56, p. 182-192.

Lucas, S. G., Kietzke, K. K., and Hunt, A. P., 1985, The Jurassic System in east-central New Mexico: New Mexico Geological Society, Guidebook 36, p. 213-243.

Lucas, S. G., Zeigler, K. E., Heckert, A. B., and Hunt, A. P., 2003, Upper Triassic stratigraphy and biostratigraphy, Chama basin, north-central New Mexico: New Mexico Museum of Natural History and Science, Bulletin 24, p. 15-39.

Lucas, S. G., Zeigler, K. E., Heckert, A. B., and Hunt, A. P., 2005b, Review of Upper Triassic stratigraphy and biostratigraphy in the Chama basin, northern New Mexico: New Mexico Geological Society, Guidebook 56, p. 170-181.

Lucas, S. G., Harris, S. K., Spielmann, J. A., Berman, D. S., Henrici, A. C., Heckert, A. B., Zeigler, K. E. and Rinehart, L. F., 2005c, Early Permian vertebrate assemblage and its biostratigraphic significance, Arroyo del Agua, Rio Arriba County, New Mexico: New Mexico Geological Society, Guidebook 56, p. 288-296.

Maldonado, Florian, 2008, Geologic map of the Abiquiu quadrangle, Rio Arriba County, New Mexico: U.S. Geological Survey Scientific Investigations Map 2998, 1 sheet, scale 1:24,000, 1 pamphlet, 21 p.

Maldonado, F. and Kelley, S.A., 2009, Revisions to the stratigraphic nomenclature of the Abiquiu Formation, Abiquiu and contiguous areas, north-central New Mexico, New Mexico Geology, v. 31, no. 1, p. 3-8.

Saucier, A. E., 1974, Stratigraphy and uranium potential of the Burro Canyon Formation in the southern Chama Basin, New Mexico: New Mexico Geological Society, Guidebook 25, p. 211-217.

Smith, C. T., Budding, A. J. and Pitrat, C. W., 1961, Geology of the southeastern part of the Chama basin: New Mexico Bureau of Mines and Mineral Resources, Bulletin 75, 57 p.

Smith, G.A., Moore, J.D., and McIntosh, W.C., 2002, Assessing roles of volcanism and basin subsidence in causing Oligocene–lower Miocene sedimentation in the northern Rio Grande Rift, New Mexico, U.S.A.: Journal of Sedimentary Research, v. 72, p. 836–848.

Stewart, J.H., Poole, F.G. and Wilson, R.F., 1972, Stratigraphy and origin of the Chinle Formation and related Upper Triassic strata of the Colorado Plateau region: U.S. Geological Survey Professional Paper 690, 336 p.

Timmer, R., Woodward, L., Kempter, K., Kelley, S., Osburn, R., Osburn, M., Buffler, R., and Lawrence, J.R., 2006, Preliminary Geologic Map of the Jarosa Quadrangle, Rio Arriba County, New Mexico: New Mexico Bureau of Geology and Mineral Resources Open-File Geologic Map OF-GM-128, scale 1:24,000, 1 sheet.

Wood, G.H. and Northrop, S.A., 1946, Geology of the Nacimiento Mountains, San Pedro Mountain, and adjacent plateaus in parts of Sandoval and Rio Arriba Counties, New Mexico: U.S. Geological Survey, Oil and Gas Investigations Map OM-57.

Appendix I

Cutler Group measured section, El Cobre Canyon

Measured along the western floor and wall of El Cobre Canyon in secs. 25-26, T24N, R5E. Base at UTM Zone 13, 378369E, 4016319 (NAD27) and top at 376985E, 4016278N. Strata dip 8° to S40°W.

Unit lithology	Thickness (m)
Upper Triassic:	
Chinle Group:	
Shinarump Formation:	
85. Conglomeratic sandstone; very pale orange (10YR8/2) and moderate yellowish brown (10YR5/4); quartzose; coarse grained; not calcareous; clasts are chert, jasper and quartzite pebbles; trough crossbedded. Not measured.	
Unconformity	
Permo-Pennsylvanian, Cutler Group:	
Arroyo del Agua Formation	
84. Sandy siltstone; mottled pale red (10R6/2) and light greenish gray (5GY8/1); not calcareous; blocky.	1.5
83. Sandy siltstone; same as unit 75.	6.0
82. Sandstone; yellowish gray (5Y8/1) and moderate reddish brown (10R4/6); arkosic; coarse grained; not calcareous; trough crossbedded; bench.	3.4
81. Sandy siltstone; moderate reddish brown (10R4/6); micaceous; not calcareous.	1.3
80. Sandy siltstone; same as unit 75.	6.0
79. Sandstone; same as unit 76.	3.3
78. Calcrete pebble conglomerate; pale yellowish brown (10YR6/2) and light olive gray (5Y6/1); bench.	0.7
77. Sandy siltstone; same as unit 75.	4.5
76. Sandstone; moderate reddish brown (10R4/6) and pale reddish brown (10R5/4); arkosic; coarse grained; not calcareous; trough crossbedded; multistoried.	2.6
75. Sandy siltstone; moderate reddish brown (10R4/6); slightly calcareous; some calcrete nodules; slope.	27.0
74. Sandstone; moderate reddish brown (10R4/6); arkosic; coarse grained; trough crossbeded.	1.5
73. Muddy siltstone; moderate reddish brown (10R4/6); calcrete nodules.	14.0
72. Conglomeratic sandstone; pale reddish brown (10R5/4) and moderate reddish brown (10R4/6); arkosic; coarse grained; conglomerate is siltstone and calcrete rip-ups; trough crossbedded; scour base; multistoried bench.	5.7
71. Muddy siltstone; same as unit 73.	5.2
70. Sandstone; yellowish gray (5Y8/1) and moderate reddish brown (10R4/6); arkosic; coarse grained; calcareous; trough crossbedded; multistoried.	2.8
69. Sandstone; moderate reddish brown (10R4/6); arkosic; micaceous;	

	coarse grained; slightly calcareous; in ledges (0.3-m thick) separated by blocky siltstone like unit 68; some calcrete.	6.0
68.	Sandy siltstone; same as unit 60; many calcrete nodules.	7.0
67.	Sandstone; same as unit 63.	2.0
66.	Sandy siltstone; same as unit 60.	6.0
65.	Conglomeratic sandstone; sandstone is light greenish gray (5GY8/1) and moderate reddish brown (10R4/6); arkosic, coarse grained and calcareous; clasts are calcrete pellets; trough crossbedded.	1.2
64.	Sandy siltstone; same as unit 60.	1.6
63.	Sandstone; pale reddish brown (10R5/4) and moderate reddish brown (10R4/6); arkosic; coarse grained; trough crossbedded; scour base with 3 m of relief.	6.0
62.	Sandy siltstone; same as unit 60.	0.8
61.	Sandstone; same as unit 61.	0.7
60.	Sandy siltstone; moderate reddish brown (10R4/6); not calcareous; blocky; calcrete nodules.	4.6
59.	Sandy siltstone; same as unit 54; abundant calcrete.	4.0
58.	Sandstone; moderate reddish brown (10R4/6); arkosic; coarse to very coarse grained; calcareous; some calcrete pebbles; trough crossbedded; scour base locally cuts down to unit 55.	3.0
57.	Sandy siltstone; grayish red (10R4/2); calcareous; blocky.	1.0
56.	Sandy siltstone; same as unit 54.	6.2
55.	Sandstone; pebbly at base; moderate reddish brown (10R4/6) and pale red (10R6/2); arkosic; coarse to very coarse grained; calcareous; pebbles are siltstone and calcrete rip ups; trough crossbedded; bench.	1.7
54.	Sandy siltstone; moderate reddish brown (10R4/6); calcareous; blocky.	8.7
El Cobre Canyon Formation:		
53.	Sandstone; pale reddish brown (10R5/4); fine grained; arkosic; very calcareous; laminar and bioturbated.	1.7
52.	Sandy siltstone; same as unit 44.	1.6
51.	Sandstone; same as unit 47.	0.6
50.	Sandy siltstone; same as unit 44.	0.2
49.	Sandstone; same as unit 47.	0.3
48.	Sandy siltstone; same as unit 44.	1.0
47.	Sandstone; pale reddish brown (10R5/4) and grayish red (10R4/2); fine grained; arkosic; calcareous; massive.	0.8
46.	Sandy siltstone; same as unit 44.	1.5
45.	Sandstone; pale reddish brown (10R5/4); arkosic; fine grained; calcareous; bioturbated.	0.6
44.	Sandy siltstone; pale reddish brown (10R5/4); calcareous; calcrete; blocky.	2.0
43.	Conglomeratic sandstone; pale reddish brown (10R5/4); coarse to very coarse grained; arkosic; clasts are quartzite and calcrete pebbles; very calcareous; trough crossbedded; scour base; bench.	2.7
42.	Sandy siltstone; same as unit 44 except laminar.	1.8
41.	Sandy siltstone; same as unit 44.	7.3

40.	Sandstone; same as unit 38.	0.6
39.	Sandy siltstone; same as unit 44.	3.8
38.	Sandstone; pinkish gray (5YR8/1) and light brownish gray (5YR6/1); arkosic; coarse grained; very calcareous; ripple laminated.	0.3
37.	Sandy siltstone; pale reddish brown (10R5/4); abundant calcrete nodules; blocky; slope.	2.7
36.	Sandstone; same as unit 38; thin bioturbated ledge.	1.8
35.	Sandy siltstone; same as unit 37; some thin sandstone lenses like unit 38.	3.2
34.	Sandstone; same as unit 32.	0.5
33.	Sandy siltstone; same as unit 31.	1.0
32.	Sandstone; pinkish gray (5YR8/1) and light olive gray (5Y6/1); arkosic; calcareous; coarse grained; bioturbated.	1.0
31.	Sandy siltstone; pale reddish brown (10R5/4); micaceous; numerous calcrete nodules; blocky slope; a few lenses of sandstone like unit 32.	4.0
30.	Sandstone; yellowish gray (5Y8/1) and light olive gray (5Y6/1); arkosic; coarse grained; calcareous; trough crossbedded.	3.5
29.	Sandstone; same as unit 27, bench.	2.9
28.	Sandy siltstone; pale red (10R6/2) and pale reddish brown (10R5/4); laminar; calcareous.	0.8
27.	Sandstone; yellowish gray (5Y8/1); arkosic; coarse grained; very calcareous; trough crossbedded; bench.	2.9
26.	Sandy shale; light olive gray (5Y6/1); not calcareous; plant debris.	2.5
25.	Conglomeratic sandstone; yellowish gray (5Y8/1) and moderate orange pink (10R7/4); arkosic; coarse grained; very calcareous; clasts are quartzite up to 6 cm diameter; trough crossbedded.	1.9
24.	Sandy siltstone; same as unit 18.	1.6
23.	Calcrete ledge; light olive gray (5Y6/1); some associated calcrete-pebble conglomerate.	1.3
22.	Sandy siltstone; same as unit 18; blocky; slope.	3.1
21.	Calcrete ledge; same as unit 23.	0.1
20.	Sandy siltstone; same as unit 18.	0.7
19.	Sandstone; pale red (10R6/2); arkosic; fine grained; very calcareous; massive; cuesta.	0.6
18.	Sandy siltstone; pale reddish brown (10R5/4); micaceous; not calcareous; numerous rhizoliths.	7.5
17.	Conglomerate; light olive gray (5Y6/1); calcrete pebbles in coarse-grained arkosic sandstone matrix; trough crossbedded; bench.	1.6
16.	Sandy siltstone; same as unit 18.	3.3
15.	Sandstone; same as unit 6.	0.2
14.	Sandy siltstone; same as unit 7.	1.9
13.	Sandstone; yellowish gray (5Y8/1) and moderate orange pink (10R7/4); arkosic; coarse grained; calcareous; trough crossbedded; multistoried bench.	2.4
12.	Sandy siltstone; same as unit 7 except trough crossbedded.	2.2
11.	Sandy siltstone; same as unit 7.	5.0

10. Sandstone; pale reddish brown (10R5/4); arkosic; coarse grained; not calcareous; trough crossbedded; top surface has desiccation tracks. 1.2
9. Sandy siltstone; same as unit 7. 2.2
8. Sandstone; pale reddish brown (10R5/4); arkosic; medium grained; very calcareous; some calcrete rip-ups; trough crossbedded; multistoried bench. 2.0
7. Sandy siltstone; grayish red (10R4/2) and pale reddish brown (10R5/4); micaceous; not calcareous; abundant rhizoliths. 1.6
6. Sandstone; light olive gray (5Y6/1); arkosic; micaceous; medium grained; calcareous; ripple laminated. 0.4
5. Conglomerate; light olive gray (5Y6/1); calcrete pebbles and a sparse matrix of arkosic sand grains; bench. 0.2
4. Sandy siltstone; pale reddish brown (10R5/4) and grayish red (10R4/2); micaceous; not calcareous; laminar. 5.5
3. Conglomeratic sandstone; same as unit 1. 3.2
2. Sandy siltstone; pale reddish brown (10R5/4); micaceous; calcareous; blocky. 7.7
1. Conglomeratic sandstone; pale reddish brown (10R5/4); arkosic; micaceous; very calcareous; coarse grained; clasts are gray quartzite; trough crossbedded; multistoried.

Appendix II

$^{40}Ar/^{39}Ar$ Geochronology Results from Sierra Negra and Cerrito de la Ventana, Rio Arriba County

By

Lisa Peters

OCTOBER 15 , 2009

NEW MEXICO
GEOCHRONOLOGY RESEARCH LABORATORY
(NMGRL)

CO-DIRECTORS LABORATORY TECHNICIAN

DR. MATTHEW T. HEIZLER LISA PETERS

DR. WILLIAM C. MCINTOSH

Internal Report #: NMGRL-IR-**580**

Age Data

Three basalts from Sierra Negra and Cerrito de la Ventana in Rio Arriba County, New Mexico were submitted by Kirt Kempter as part of the state map program.

Table 1. Brief summary of results.

Sample	Phase Age±2 sigma (Ma)	Comments
SN-1 Groundmass concentrate	5.00±0.15	Well-behaved
CSE-1 Groundmass concentrate	18.1±1.2	somewhat disturbed
CSE-2 Groundmass concentrate	18.91±0.41	somewhat disturbed

$^{40}Ar/^{39}Ar$ Analytical Methods and Results

The basalts were crushed, sieved and cleaned with hydrochloric acid and rinsed with distilled water. Groundmass concentrates and monitors (Fish Canyon tuff sanidine, 28.02, Renne et al., 1998) were loaded into aluminum discs and irradiated for 7 hours at the Nuclear Science Center in College Station, Texas.
The groundmass concentrates were analyzed with the furnace incremental heating age spectrum method. Abbreviated analytical methods for the dated sample are given in Table 2, and details of the overall operation of the New Mexico Geochronology Research Laboratory is provided in the Appendix. The age results are summarized in Tables 1and 2 and the argon isotopic data are given in Table 3.

SN-1 Weighted Mean Age=5.00±0.15 Ma n/n_{total} =9/10 MSWD=1.52
SN-1 yielded a fairly well-behaved age spectrum (Figure 1a). The initial step yields an anomalously old apparent age but the following steps are nearly concordant. A weighted mean age of 5.00±0.15 Ma is calculated from this portion of the age spectrum. -2- The radiogenic yields rise over the initial 55.4% of the ^{39}Ar released from 10.3% to 38.4% and then decrease to 2.8% over the last 44.6% of the age spectrum. The K/Ca values are somewhat oscillatory with values dropping from 0.27 to 0.16 over the first 38.2% of the ^{39}Ar released and then rising again slightly (0.23) until the last 12.9% of the age spectrum where the K/Ca value drops to 0.031. Inverse isochron analysis of steps B-I yields an age of 5.06±0.23 Ma with an atmospheric intercept of 294.0±3.7 (Figure 1b).

CSE-1 Weighted Mean Age=18.1±1.2 Ma n/n_{total} =4/10 MSWD=10.58
CSE-1 yielded a disturbed slightly hump-shaped age spectrum (Figure 2a). Radiogenic yields are low (<10%) over the initial 37.4% of the age spectrum. These low radiogenic yields result in high errors on the low temperature heating steps. After this portion of the age spectrum, the apparent ages drop (20.2 Ma to 17.07 Ma), while the

radiogenic yields rise to 38.2% radiogenic before dropping again to 9.8%. The K/Ca values are roughly correlative with the radiogenic yields rising from 0.44 to 0.65 over 55.7% of the age spectrum and then dropping to 0.028. A weighted mean age of 18.10±1.18 Ma is calculated from steps F-I. These steps are not concordant; the MSWD value is 10.58. An isochron age of 18.0±1.1 Ma (Figure 2b) is calculated from steps A-H, this age has a $^{40}Ar/^{36}Ar$ intercept of 299.1±3.1, almost within error of the atmospheric ratio (295.5).

CSE-2 Weighted Mean Age=18.91±0.41 Ma n/n_{total} =8/10 MSWD=14.14
CSE-2 yielded a somewhat disturbed hump-shaped age spectrum (Figure 3a). The initial two steps yield anomalously young (12.3 Ma and 13.09 Ma) apparent ages. The following steps, while not concordant yield older apparent ages ranging from 17.91 Ma to 19.9 Ma. A weighted mean age of 18.91±0.41 Ma is calculated from these steps, we note that the MSWD value for this age is quite high, 14.14. A value over 2.18 indicates that the error is not due to analytical error alone. The radiogenic yields increase from 1.2% to 59.3% over the initial 18.8% of the age spectrum and then remain fairly constant until the final heating step where the radiogenic yield drops to 10.8%. The K/Ca values are correlative with the radiogenic yields, increasing from 0.35 to 0.90 and then remaining fairly constant until the final two steps where they drop as low as 0.044. Isochron analysis of steps C-J yield an isochron age of 18.83±0.85 Ma, these steps yield an atmospheric intercept of 297.1±19.0 with an MSWD of 16.3 (Figure 3b).

Discussion

We note that the age spectrum for sample SN-1 is nearly concordant with over 99% of the ^{39}Ar released being used to calculate the weighted mean age (5.00±0.15 Ma). The age spectrum for SN-1 provides a precise, reliable eruption age; one of much higher quality than the age spectra generated for the other two samples from this project. As noted above, the results from CSE-1 and CSE-2 are of much lower quality than SN-1 but probably provide approximate eruption ages. We suspect that samples CSE-1 and CSE-2 have been affected to different degrees by ^{39}Ar recoil and alteration and accompanying Ar loss, the affect of these on an age spectrum is explained in Figure 4. Basaltic samples that have undergone alteration to low K phases such as clays are susceptible to ^{39}Ar recoil. During ^{39}Ar recoil, the ^{39}Ar created at the reactor is redistributed from high K phases to low K phases. Samples suspected of having undergone recoil are usually assigned the integrated age as the best estimate of the sample's age. Although we suspect CSE-1 has undergone recoil, the extremely old first step (101.4 Ma) results in the integrated age being ~4 Ma older than the weighted mean age calculated from the rest of the age spectrum. We have therefore, decided to assign the weighted mean age calculated from the age spectrum as the preferred age of this sample. We note that the inverse isochron for this sample suggests that there may be slight excess argon. The young apparent ages correlated with low radiogenic yields revealed in the early steps of CSE-2 are suggestive of Ar loss (which would lower the integrated age of sample) so we are hesitant to assign the integrated age as the eruption age of CSE-2. For this reason we have assigned the weighted mean age (18.91±0.41 Ma) as our best estimate of this samples eruption age.